

Storage properties of Ce³⁺ doped haloborate phosphors enriched with ¹⁰B isotope

A. V. Sidorenko, A. J. J. Bos, P. Dorenbos, C. W. E. van Eijk, P. A. Rodnyi et al.

Citation: *J. Appl. Phys.* **95**, 7898 (2004); doi: 10.1063/1.1719260

View online: <http://dx.doi.org/10.1063/1.1719260>

View Table of Contents: <http://jap.aip.org/resource/1/JAPIAU/v95/i12>

Published by the [American Institute of Physics](#).

Related Articles

Synthesis and phosphorescence mechanism of a reddish orange emissive long afterglow phosphor Sm³⁺-doped Ca₂SnO₄

Appl. Phys. Lett. **98**, 121906 (2011)

Correlations between low temperature thermoluminescence and oxygen vacancies in ZnO crystals

J. Appl. Phys. **109**, 053508 (2011)

Color tunable phosphorescence in KY₃F₁₀:Tb³⁺ for x-ray or cathode-ray tubes

J. Appl. Phys. **106**, 034915 (2009)

Thermoluminescence properties of carbon doped Y₃Al₅O₁₂ (YAG) crystal

J. Appl. Phys. **106**, 033105 (2009)

Characterization of unswept and swept quartz crystals for space applications

J. Appl. Phys. **105**, 113523 (2009)

Additional information on *J. Appl. Phys.*

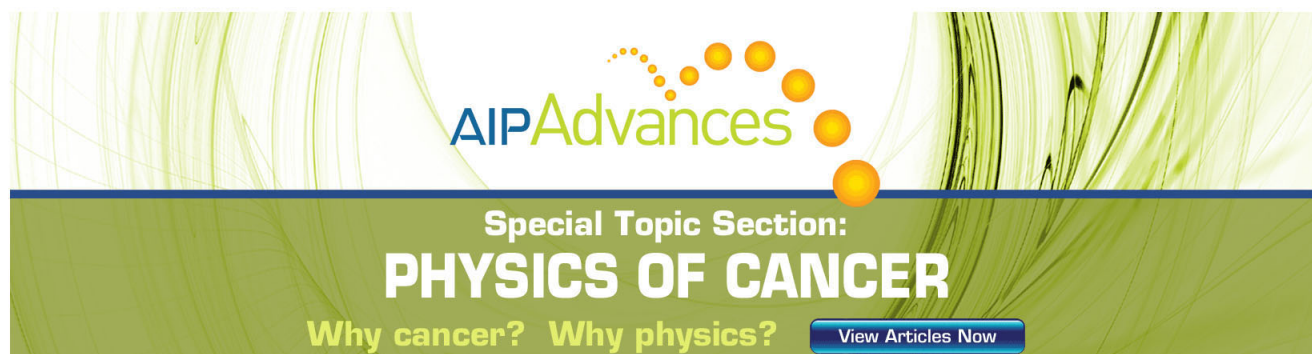
Journal Homepage: <http://jap.aip.org/>

Journal Information: http://jap.aip.org/about/about_the_journal

Top downloads: http://jap.aip.org/features/most_downloaded

Information for Authors: <http://jap.aip.org/authors>

ADVERTISEMENT



AIPAdvances

Special Topic Section:
PHYSICS OF CANCER

Why cancer? Why physics? [View Articles Now](#)

Storage properties of Ce^{3+} doped haloborate phosphors enriched with ^{10}B isotope

A. V. Sidorenko, A. J. J. Bos, P. Dorenbos, and C. W. E. van Eijk
Interfaculty Reactor Institute, Delft University of Technology, Delft, The Netherlands

P. A. Rodnyi
St. Petersburg State Technical University, St. Petersburg, Russian Federation

I. V. Berezovskaya and V. P. Dotsenko
A. V. Bogatsky Physico-Chemical Institute, Ukrainian Academy of Science, Kharkov, Ukraine

A. I. Popov
Service Detecteurs De Neutrons, Institut Laue-Langevin, Grenoble, France

(Received 9 February 2004; accepted 8 March 2004)

In this work we investigated the suitability of newly synthesized series of haloborate phosphors with the general formula $M_2B_5O_9X:\text{Ce}^{3+}$ ($M = \text{Sr}$ or Ca ; $X = \text{Br}$ or Cl) for thermal neutron detection and with reduced sensitivity to γ background. Storage properties such as yield of photostimulated luminescence (PSL) and thermoluminescence are reported. Based on these results the series of the haloborates with 99% enrichment of ^{10}B was sensitized to increase neutron sensitivity. The PSL yields of enriched with ^{10}B haloborates were compared with a common mixture of $\text{BaFBr}:\text{Eu}^{2+}$ (40 wt %) and Gd_2O_3 (60 wt %) under γ and neutron irradiation. The PSL light yield from $\text{Ca}_2^{10}\text{B}_5\text{O}_9\text{Cl}:\text{Ce},\text{Na}$ phosphor after neutron irradiation is 16 times less than that from $\text{BaFBr}:\text{Eu}^{2+}x\text{Gd}_2\text{O}_3$. However, the neutron to γ discrimination of $\text{Ca}_2^{10}\text{B}_5\text{O}_9\text{Cl}:\text{Ce},\text{Na}$ (1%) is almost an order of magnitude better than that of $\text{BaFBr}:\text{Eu}^{2+}x\text{Gd}_2\text{O}_3$. Therefore, haloborate phosphors should be more suitable when utilized in environments with a high γ background.

© 2004 American Institute of Physics. [DOI: 10.1063/1.1719260]

I. INTRODUCTION

Imaging of x rays and γ rays with image plates (IP) based on detection of photostimulated luminescence (PSL) from storage phosphors is widely applied. The storage phosphor used nowadays in almost all the commercial imaging systems is $\text{BaSrF}(\text{Br},\text{I}):\text{Eu}^{2+}$. Applications based on imaging of thermal neutrons are less known. Neutron sensitive IPs as position sensitive detectors are successfully applied in several neutron applications. Recent data from neutron diffractometer designed at Institute of Laue-Langevin are a very good example of it.¹

The most common neutron IP is based on a $\text{BaFBr}:\text{Eu}^{2+}x\text{Gd}_2\text{O}_3$ mixture (Gd-IP). However, this phosphor is rather sensitive to γ -ray background, which reduces the image quality. Therefore, the main priority for optimization neutron IP is to reduce the γ -ray sensitivity. Two ways to reduce the γ sensitivity can be proposed. In a first approach, the neutron converter is chosen in such a way that the number of created PSL active defects from incident neutrons is much higher than that from γ rays. For example, if ^{10}B is used, the energy of secondary particles after neutron capture, which is about 2.78 MeV is much higher than the energy deposition from captured γ -ray with energy of several hundreds of keV.

The second approach implies that Z_{eff} of the storage phosphor is chosen as low as possible. The γ -ray background in the experimental hall and in the neutron beam is mainly determined by γ -ray energies below 2 MeV. Therefore the

main process of γ -ray interaction with a high- Z_{eff} material is a photoelectric effect, and the cross section of this process decreases significantly with Z_{eff} of a material. Thus a search of new neutron storage phosphors must be done among materials with low Z_{eff} .

When both approaches are combined, i.e., low- Z_{eff} material with a ^{10}B or ^6Li neutron converter, the lowest γ -ray sensitivity in comparison to neutrons is expected. Theoretical calculations show that with storage phosphors having a neutron sensitive element in its crystal lattice, a higher detective quantum efficiency can be achieved.²

There are several elements, such as Gd, ^6Li , and ^{10}B , that can be used as a neutron converter. In spite of the highest neutron capture cross section, a Gd-based neutron converter or storage phosphor is not favorable because of low kinetic energy of secondary particles.² The choice of ^6Li or ^{10}B is a compromise between higher neutron capture cross section and energy deposition into the phosphor from secondary radiation.

In this work storage properties of the series of haloborates with general formula $M_2B_5O_9X:\text{Ce}^{3+}$, A^+ ($M = \text{Ba}, \text{Sr}, \text{Ca}, X = \text{Cl}, \text{Br}, A = \text{Na}^+, \text{K}^+$) and natural abundance of ^{10}B isotope have been investigated upon β , γ , and neutron irradiation. The natural abundance of ^{10}B is 18.8%. Since only ^{10}B has a high neutron capture cross section (3840 b for a 1.8 Å neutron) the series of the haloborates with 99% enrichment of ^{10}B was sensitized afterwards to increase a sensitivity to thermal neutrons. The enriched samples were compared with $\text{BaFBr}:\text{Eu}^{2+}x\text{Gd}_2\text{O}_3$ mixture.

TABLE I. Summary of TL and PSL yields of investigated compounds. All the samples were measured at the same conditions. Irradiation was performed with $^{90}\text{Sr}/^{90}\text{Y}$ β source. The fourth column shows TL yields measured with a U-340 filter. This filter is used for PSL measurements with blue LEDs, and the fifth column represents the attenuation of the emission light from the sample passing through the U-340 filter. The sixth column shows the integral PSL signal during 20 s of photostimulation with $\lambda = 470$ nm.

Compound	Concentration (mol %)	Total TL intensity (arbitrary units)	TL intensity U-340 (arbitrary units)	Ratio TL/TL _{U-340}	PSL intensity (arbitrary units)
$\text{Sr}_2 \text{ natB}_5\text{O}_9\text{Br}:\text{Ce}^{3+}$	1%	24.3	6.5	3.8	5.8
$\text{Sr}_2 \text{ natB}_5\text{O}_9\text{Br}:\text{Ce}^{3+}, \text{Na}^+$	1%, 1%	61.5	23.0	2.7	12
$\text{Sr}_2 \text{ natB}_5\text{O}_9\text{Br}:\text{Ce}^{3+}, \text{K}^+$	1%, 1%	55.8	14.3	3.9	9.9
$\text{Sr}_2 \text{ natB}_5\text{O}_9\text{Cl}:\text{Ce}^{3+}$	0.5%	22.6	7.7	2.9	5.4
$\text{Sr}_2 \text{ natB}_5\text{O}_9\text{Cl}:\text{Ce}^{3+}, \text{Na}^+$	0.5%, 0.5%	47.8	26.7	1.8	15
$\text{Ca}_2 \text{ natB}_5\text{O}_9\text{Br}:\text{Ce}^{3+}$	1%	31.2	6.6	4.8	5.5
$\text{Ca}_2 \text{ natB}_5\text{O}_9\text{Br}:\text{Ce}^{3+}, \text{Na}^+$	0.5%	25.8	9.3	2.8	6.5
$\text{Ca}_2 \text{ natB}_5\text{O}_9\text{Cl}:\text{Ce}^{3+}, \text{Na}^+$	1%	31.9	14.6	2.2	9.4
$\text{Sr}_2 \text{ }^{10}\text{B}_5\text{O}_9\text{Br}:\text{Ce}^{3+}$	1%		6.7		3.7
$\text{Sr}_2 \text{ }^{10}\text{B}_5\text{O}_9\text{Br}:\text{Ce}^{3+}, \text{K}^+$	1%, 1%		7.2		4.8
$\text{Sr}_2 \text{ }^{10}\text{B}_5\text{O}_9\text{Br}:\text{Ce}^{3+}, \text{Na}^+$	1%, 1%		7.1		4.5
$\text{Ca}_2 \text{ }^{10}\text{B}_5\text{O}_9\text{Br}:\text{Ce}^{3+}, \text{Na}^+$	1%, 1%		6.2		3.7
$\text{Ca}_2 \text{ }^{10}\text{B}_5\text{O}_9\text{Cl}:\text{Ce}^{3+}, \text{Na}^+$	1%, 1%		8.3		6.1

II. EXPERIMENT

The solid solutions of haloborates $M_2\text{B}_5\text{O}_9\text{X}:\text{Ce}^{3+}$ ($M = \text{Ca}, \text{Sr}, \text{Ba}; \text{X} = \text{Cl}, \text{Br}$) were prepared in A. V. Bogatsky Physico-Chemical Institute using a standard solid state method as described in Ref. 3. As starting mixtures MCO_3 , $\text{MX}_2 \cdot n\text{H}_2\text{O}$ (10% excess), $\text{Ce}(\text{NO}_3)_3$, and $\text{H}^{\text{nat}}\text{BO}_3$ (15% of excess) were used. For preparation of the samples with enriched abundance of ^{10}B , boron oxide with 99% of ^{10}B was used. As a reference material for comparative measurements the mixture of $\text{BaFBr}:\text{Eu}^{2+}$ (40 wt %) with Gd_2O_3 (60 wt %) was used.

The measurements of thermostimulated and photostimulated luminescence intensities of the series of haloborates were performed with the help of Risø-TL/PSL-DA-15A/B reader with installed $\text{Sr}^{90}/\text{Y}^{90}$ β source with a dose rate 1.0 mGy/s in air. As a photostimulation source a ring of blue light emitting diodes (Blue LEDs) with $\lambda = 470 \pm 20$ nm was used. A set of three U-340 filters ($\lambda_p \sim 340$ nm, FWHM) (full width at half maximum) ~ 80 nm) with total thickness 7 nm was employed in order to shield the photomultiplier tube (PMT) window from the scattered light of the stimulation source.

The comparison of PSL yields of haloborates and $\text{BaFBr}:\text{Eu}^{2+}x\text{Gd}_2\text{O}_3$ was done with a single-grain attachment to the Risø-TL/PSL reader, which was originally designed to measure sand-sized grains.⁴ This system was chosen because of read-out conditions, which are very similar to those in commercial image plate scanners. As a photostimulation source a 10 mW Nd:YVO₄ solid state diode-pumped laser was used, emitting at 532 nm and producing a spot ≈ 120 μm in diameter at the surface of the sample disk. In our PSL experiments we set 10% of the full laser power, i.e., 1 mW. A small portion of powder sample was put into the surface of 10 mm diameter aluminum disk. The thickness of the powder layer is about 300 μm . The laser beam can scan the disk in 10×10 grid pattern giving a total of 100 pixels of photostimulated phosphor on each sample disk.

Each pixel was read-out during 2 s, and the PSL signal was recorded in an array of 100 channel. The value of the first channel represents the detected PSL signal in the first 20 ms of laser stimulation. The PSL yields of studied phosphors were characterized by this value.

Irradiation by neutrons was performed using one of the beam lines (L21) of the IRI nuclear research reactor. The energy spectrum of thermal neutrons is close to a Maxwell distribution with a maximum at 25 meV. The neutron flux was measured to be about $5 \times 10^4 \text{ cm}^{-2} \text{ s}^{-1}$. Irradiation by γ rays was performed with a ^{137}Cs source (662 keV) with a dose rate ~ 2 mGy/h.

III. EXPERIMENTAL RESULTS AND DISCUSSION

A. TL and PSL study of haloborates with natural abundance of ^{10}B (18.8%)

We have presented the luminescence and thermoluminescence studies of $\text{Sr}_2\text{B}_5\text{O}_9\text{Br}$ doped with Ce^{3+} in.⁵ It was established that increase of Ce^{3+} concentration leads to an increase of TL yield and the optimum is between 1% and 2%. Introduction of K^+ or Na^+ codopants leads to an increase of the TL yield as well, what can be explained by higher solubility of Ce^{3+} ions in the lattice in the presence of monovalent charge compensating codopants.

The measured TL yields of the series of β -irradiated haloborates with natural abundance of ^{10}B and different types of anions and cations as well as monovalent codopants are listed in column 3 of Table I. All the samples exhibit a TL yield of the same order of magnitude. The TL glow curves of $\text{Sr}_2\text{B}_5\text{O}_9\text{Br}:\text{Ce}^{3+}, \text{Na}^+$, $\text{Sr}_2\text{B}_5\text{O}_9\text{Br}:1\% \text{Ce}^{3+}$, and $\text{Ca}_2\text{B}_5\text{O}_9\text{Cl}:\text{Ce}^{3+}, \text{Na}^+$ are shown in Figs. 1(a–c) (solid curves). The intensity of the low temperature peak at 350 K relative to that at high temperature 400–430 K is much higher in the presence of monovalent codopants.

Emission bands of Ce^{3+} luminescence in haloborates are located in the 325–360 nm region depending on cation and

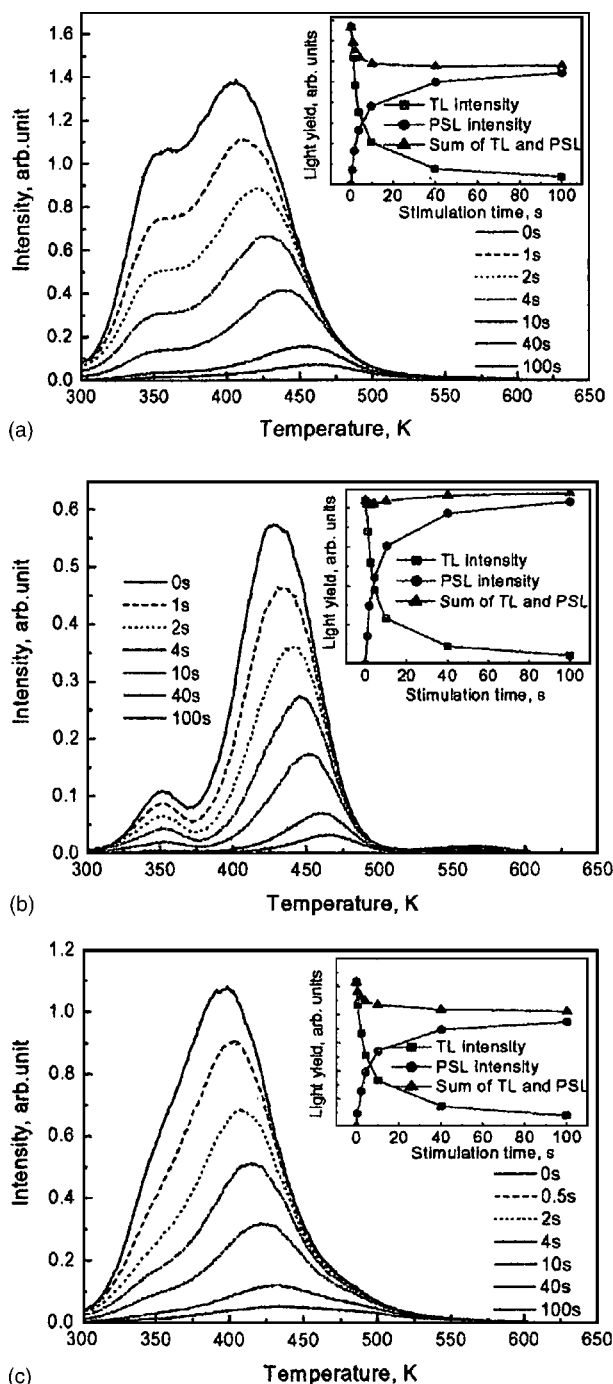


FIG. 1. The TL glow curves of β irradiated $\text{Sr}_2\text{B}_5\text{O}_9\text{Br}:\text{Ce}^{3+}, \text{Na}^+$ (a), $\text{Sr}_2\text{B}_5\text{O}_9\text{Br}:1\% \text{Ce}^{3+}$ (b), and $\text{Ca}_2\text{B}_5\text{O}_9\text{Cl}:\text{Ce}^{3+}, \text{Na}^+$ (c), which were recorded after photostimulation of different duration—from 0 to 100 s. Blue LED's ($\lambda = 470$ nm) were used as a stimulation source. The TL curves were recorded with a heating rate of 1 K/s. Irradiation was performed with $^{90}\text{Sr}/^{90}\text{Y}$ β source. In the inset integral intensity of residual TL signal, PSL signal measured before TL measurements, and the sum of both are plotted as a function of optical stimulation time.

anion type. The so-called stimulation spectrum of photostimulated luminescence of $\text{Sr}_2\text{B}_5\text{O}_9\text{Br}:1\% \text{Ce}^{3+}$ is shown in Fig. 2 (solid curve). The spectrum was recorded after γ irradiation of the sample and detecting Ce^{3+} luminescence at 350 nm. The spectrum is almost structureless and increases monotonically with shortening of the wavelength. All the studied haloborates show similar behavior of stimulation

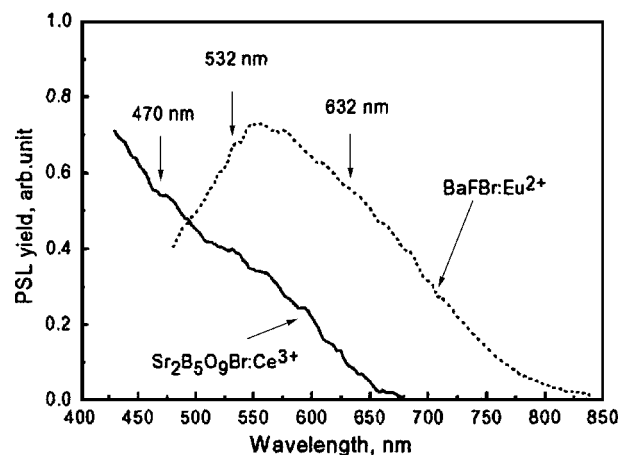


FIG. 2. PSL stimulation spectra of $\text{Sr}_2\text{B}_5\text{O}_9\text{Br}:1\% \text{Ce}^{3+}$ (solid curve) measured at $\lambda = 350$ nm emission and of $\text{BaFBr}:\text{Eu}^{2+}$ (dotted curve) measured at $\lambda = 390$ nm emission. The spectra were corrected for the intensity of the xenon lamp.

spectrum. It is seen that stimulation with the common He-Ne laser wavelength $\lambda = 632$ nm is inefficient. Applying a stimulation source with shorter wavelength down to 430 nm can increase the stimulation efficiency.

In our experiments as a stimulation source Blue LEDs with $\lambda = 470$ nm installed in the Risø reader was chosen and a pack of three U-340 cutoff filters was placed in front of the PMT. The measured TL yields with U-340 filters are listed in column 4 of Table I. The degree of attenuation of a TL signal due to the mismatch of cutoff filter transmission spectrum and the TL emission spectrum is shown in column 5 of Table I. For some compounds, especially with a high concentration of Ce^{3+} the use of U-340 filters cut off a significant part of the PSL light. For example, for $\text{Ca}_2\text{B}_5\text{O}_9\text{Br}:\text{Ce}^{3+}$ only one-fifth part of PSL light passes through the filter. With the increase of Ce^{3+} concentration the emission spectrum of Ce^{3+} luminescence shifts more to the long wavelength part. The origin of this shift has been discussed in Ref. 5.

The results of Table I show that for some samples there is a discrepancy between TL and PSL response. Especially it is pronounced for compounds codoped with Na^+ . Different recombination processes occurring upon thermal and optical stimulation can explain this.

A combined PSL and TL technique was applied to investigate the observed differences between PSL and TL signals. The procedure of this technique is as follows. After β irradiation the integral PSL signal was measured during a certain stimulation time. Immediately after photostimulation the residual TL glow curve was recorded. The residual TL signal is proportional to the number of trapped carriers, which were not released upon the preceding photostimulation. Varying the duration of the photostimulation time, information about efficiency of photostimulation of certain types of traps can be extracted. In Fig. 1 the results are shown for $\text{Sr}_2\text{B}_5\text{O}_9\text{Br}:\text{Ce}^{3+}, \text{Na}^+$, $\text{Sr}_2\text{B}_5\text{O}_9\text{Br}:\text{Ce}^{3+} 1\%$, and $\text{Ca}_2\text{B}_5\text{O}_9\text{Cl}:\text{Ce}^{3+}, \text{Na}^+$ compounds. In the insets integral intensities of PSL, TL, and both PSL+TL signals are plotted versus the time of photostimulation applied before the TL measurements.

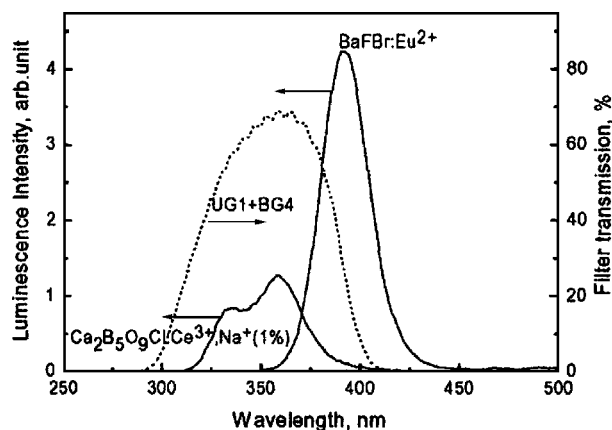


FIG. 3. Transmission spectrum of BG4 + UG1 filter (filled curve with diagonal lines), x-ray excited emission spectrum of BaFBr:Eu²⁺ phosphor and of Ca₂B₅O₉Cl:Ce³⁺, Na⁺.

For the samples with Na⁺ codoping where the intensity of 350 K TL peak is high, the integral PSL+TL signal decreases with increase of photostimulation time as it is seen in insets in Fig. 1. But after a certain stimulation time it becomes constant. We have performed the same type of experiments described above with β -irradiated samples that were annealed at 350 K, i.e., samples, in which only traps corresponding to the high temperature peak are left. In that case no decrease of integral PSL+TL signal was observed. Thus the trapped charges corresponding to the 350 K TL peak are efficiently emptied upon photostimulation, but there is non-efficient recombination with Ce³⁺ emission centers. Therefore only the traps, which correspond to the high TL peak, appear to be active in the PSL process.

B. TL and PSL study of haloborates with enriched abundance (99%) of ¹⁰B isotope

The optimal thickness of a storage phosphor layer in an image plate is not more than 150 μm .⁶ Larger thickness would not lead to PSL increase, since the created PSL photons deep inside the layer will not be able to escape from the surface of the image plate. It is easy to calculate² that for Ca₂^{nat}B₅O₉Br the probability for the thermal neutron to be captured in a 150 μm phosphor layer with grain filling factor 0.7 is 17%. This means that the detective quantum efficiency of such a detector would be very low.² As an example, the capture probability for BaFBr:Eu²⁺ (40 wt %) · Gd₂O₃ (60 wt %) mixture is about 99%. However, for the Ca₂¹⁰B₅O₉Br phosphor, i.e., 99% enrichment with ¹⁰B, almost 63% of thermal neutrons will be captured in a 150 μm phosphor layer. That is why the characteristics of the haloborates enriched with ¹⁰B isotope should be determined (Fig. 3).

Five samples of haloborates with 99% enrichment of ¹⁰B were synthesized. The TL and PSL yields of these samples were compared with those with natural abundance and the results are compiled in Table I. The TL and PSL yields of enriched haloborates are lower than those with natural abundance. Different starting materials used for synthesis can explain this. Boric acid was used for synthesis of haloborates

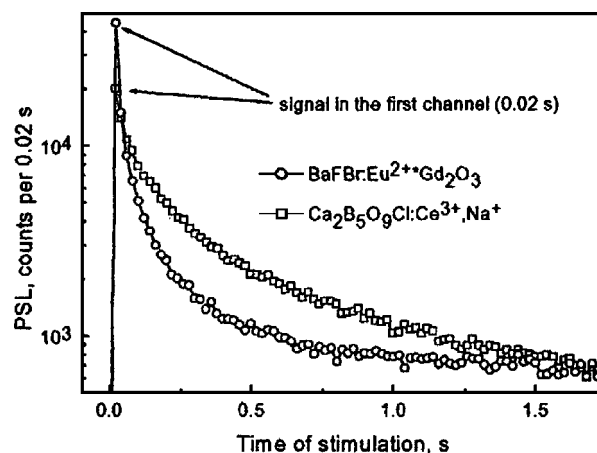


FIG. 4. The PSL curves of BaFBr:Eu²⁺·xGd₂O₃ and Ca₂¹⁰B₅O₉Cl:Ce,Na under continuous stimulation by means of Nd:YVO₄ laser ($\lambda = 532$ nm). Laser power is 1 mW and the beam diameter ≈ 120 μm on the sample surface.

with ^{nat}B and boron oxide was used for synthesis of enriched samples. The studied samples with 99% enrichment of ¹⁰B represent a “pilot” series and synthesis conditions are not yet optimized.

The results of Table I lead to the conclusion that Ca₂B₅O₉Cl:Ce³⁺, Na⁺ is the most promising of the studied series for detection of thermal neutrons with reduced sensitivity to γ rays, since it has the lowest- Z_{eff} number and, at the same time, a relatively high PSL yield.

C. Quantitative comparison of studied haloborates with BaFBr:Eu²⁺·xGd₂O₃

To perform a correct comparison between two different types of storage phosphors, the experimental conditions must be equally optimal for both of them. The read-out of BaFBr:Eu²⁺ storage phosphor is usually performed with a He-Ne laser ($\lambda = 632$ nm). However, as it can be seen from Fig. 2, the maximum of PSL excitation spectrum of BaFBr:Eu²⁺ is at 550 nm. The stimulation of haloborates is also very inefficient at $\lambda = 632$ nm. For our experiment we used a Nd:YVO₄ laser with $\lambda = 532$ nm, which is about optimal for both haloborates and BaFBr:Eu²⁺.

As a cutoff filter for protection of the PMT we used a set of BG-4 and UG-1 filters. The filters transmission curves and x-ray excited emission spectra of BaFBr:Eu²⁺, Ca₂¹⁰B₅O₉Cl:Ce³⁺, Na⁺(1%) are shown in Fig. 4. These filters attenuate the emission from BaFBr:Eu²⁺ by a factor of 5 and the emission from Ca₂¹⁰B₅O₉Cl:Ce³⁺, Na⁺ by a factor of 2.

The typical PSL curves of BaFBr:Eu²⁺·xGd₂O₃, Ca₂¹⁰B₅O₉Cl:Ce,Na upon continuous laser stimulation after neutron irradiation are shown in Fig. 4. The measurements were carried out 1 h after irradiation. The PSL signal of BaFBr:Eu²⁺ phosphor (without adding Gd₂O₃) after neutron irradiation is two orders of magnitudes lower than that of BaFBr:Eu²⁺·xGd₂O₃ or Ca₂¹⁰B₅O₉Cl:Ce,Na. Pure BaFBr:Eu²⁺ does not interact with thermal neutrons and the PSL signal is attributed to the γ rays in the neutron flux.

TABLE II. The measured PSL yields (S_n and S_γ) of some studied materials after neutron and γ irradiation. The yields are normalized to the one of BaFBr:Eu²⁺ x Gd₂O₃. The samples were measured at the same conditions.

Items	Sr ₂ ^{nat} B ₅ O ₉ Br:Ce ³⁺ (1%)	Ca ₂ ¹⁰ B ₅ O ₉ Cl:Ce,Na (1%)	BaFBr:Eu ²⁺ x Gd ₂ O ₃
S_n	3.2	6	100
S_γ (at 662 keV)	0.26	0.14	18
S_n/S_γ	12	43	5.5

The results of PSL experiments are collected in Table II. The values represent the average of PSL signals within first 20 ms of laser stimulation from 100 pixels in the sample disk. The mean measured PSL signals after neutron and γ -ray irradiation are denoted as S_n and S_γ . The values are corrected for the attenuation of the cutoff filters, i.e., the detected signal from BaFBr:Eu²⁺ x Gd₂O₃ is multiplied by 5 and that from haloborates is multiplied by 2.

The results of Table II show that the neutron sensitivity of BaFBr:Eu²⁺ x Gd₂O₃ is 16 times higher than that of Ca₂¹⁰B₅O₉Cl:Ce,Na (1%). At the same time, the γ -ray sensitivity of BaFBr:Eu²⁺ x Gd₂O₃ is 125 times higher than that of Ca₂¹⁰B₅O₉Cl:Ce,Na (1%). Thus, S_n/S_γ of Ca₂¹⁰B₅O₉Cl:Ce,Na (1%) is eight times better than that of BaFBr:Eu²⁺ x Gd₂O₃.

The fading properties of studied materials are presented in Fig. 5. It is seen that in 10 h after irradiation 46% of the initial PSL signal left in Ca₂¹⁰B₅O₉Cl:Ce,Na (1%), and this value is 77% for BaFBr:Eu²⁺ x Gd₂O₃.

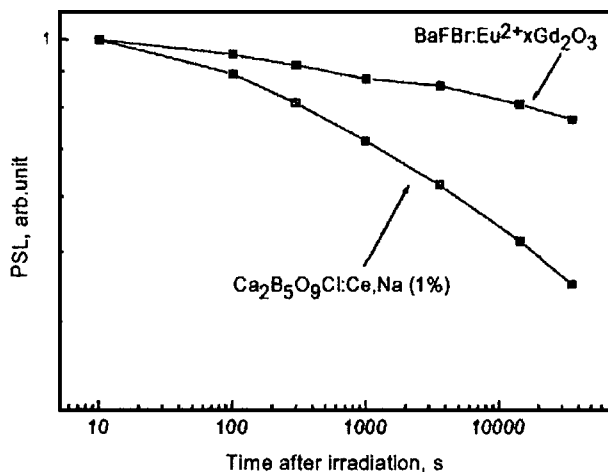


FIG. 5. Fading of PSL signal in BaFBr:Eu²⁺ x Gd₂O₃ and Ca₂B₅O₉Cl:Ce,Na (1%) at room temperature.

IV. CONCLUSIONS

The TL and PSL properties of the series of haloborates with general formula $M_2B_5O_9X:Ce^{3+},A^+$ ($M = Ba, Sr, Ca, X = Cl, Br, A = Na^+, K^+$) were studied. The results of this study brought to the conclusion that Ca₂B₅O₉Cl:Ce³⁺,Na⁺ compound is the most promising in the whole studied series for detection of thermal neutrons and with reduced sensitivity to γ rays, since it has the lowest- Z_{eff} number and, at the same time, a relatively high PSL yield. The PSL light yield from Ca₂¹⁰B₅O₉Cl:Ce,Na (1%) after neutron irradiation is 16 times less than that from BaFBr:Eu²⁺ x Gd₂O₃. However, the neutron to γ discrimination of Ca₂¹⁰B₅O₉Cl:Ce,Na (1%) is almost an order of magnitude better than that of BaFBr:Eu²⁺ x Gd₂O₃. Therefore haloborate phosphors could be more attractive when utilized in environments with a high γ background.

This is a first study of haloborates with enriched abundance of ¹⁰B isotope and improvements can be expected when further synthesis optimization is performed.

ACKNOWLEDGMENTS

This investigation was supported by the Netherlands Technology Foundation (STW) and by the IHP Contract No. HPRI-CT-1990-00040 of the European Commission.

- ¹D. A. A. Myles, C. Bon, P. Langan, F. Cipriani, J. C. Castagna, M. S. Lehmann, and C. Wilkinson, *Physica B* **241–243**, 1122 (1998).
- ²M. J. Knitel, V. R. Bom, P. Dorenbos, C. W. E. van Eijk, I. V. Berezovskaya, and V. P. Dotsenko, *Nucl. Instrum. Methods Phys. Res. A* **449**, 578 (2000).
- ³V. P. Dotsenko, I. V. Berezovskaya, N. P. Efrushina, A. S. Voloshinovskii, P. Dorenbos, and C. W. E. van Eijk, *J. Lumin.* **93**, 137 (2001).
- ⁴G. A. T. Duller, L. Bøtter-Jensen, A. S. Murray, and A. J. Truscott, *Nucl. Instrum. Methods Phys. Res. B* **155**, 506 (1999).
- ⁵A. V. Sidorenko, A. J. J. Bos, P. Dorenbos, P. A. Rodnyi, C. W. E. van Eijk, I. V. Berezovskaya, and V. P. Dotsenko, *J. Phys.: Condens. Matter* **15**, 3471 (2003).
- ⁶S. Taniguchi, A. Yamadera, T. Nakamura, and A. Fukumura, *Nucl. Instrum. Methods Phys. Res. A* **413**, 119 (1998).